Jul 1st, 12:00 AM

A Computational Study on the Influence of Urban Morphology on Wind-Induced Outdoor Ventilation

Rubina Ramponi

Bert Blocken

A Computational Study on the Influence of Urban Morphology on Wind-Induced Outdoor Ventilation

Rubina Ramponi [a,b]**, Bert Blocken** [a]
[a] *Building Physics and Services, Eindhoven University of Technology, P.O. box 513, 5600 MB Eindhoven, the Netherlands*
[b] *Building Environment Science & Technology Department, Politecnico di Milano, via Bonardi 3, 20133, Milano, Italy*
[1] *r.ramponi@tue.nl*

Abstract: Accurate modeling of urban wind flow is important for the assessment of the natural ventilation of the outdoor environment and therefore for outdoor air quality. Different geometrical levels of analysis can be used, ranging from regular arrays of obstacles to real and complex case studies. In order to avoid the complexity of real case studies and to obtain more generic results, regular arrays of obstacles represent a suitable level to study the relation between urban morphology and outdoor ventilation. This paper presents the first results of a numerical study with Computational Fluid Dynamics (CFD) of isothermal wind flow in generic urban configurations. Nine urban configurations are defined with regular arrays of obstacles by increasing the plan area density (from 0.1 to 0.6) and the frontal area density (from 0.02 to 0.45). By this variation, the flow structure varies from isolated obstacle flow over wake interference flow to skimming flow. Among the nine configurations defined, four test cases are selected for a preliminary study. 3D steady Reynolds-Averaged Navier-Stokes (RANS) CFD simulations are performed for the four selected configurations and the simulations are compared with experimental wind-tunnel data. An overall fairly good agreement is found between the experimental and numerical results obtained with RANS simulations. The results allow establishing some relationships between morphological and fluid dynamics parameters of urban wind flow and outdoor ventilation. It is found that the upstream building density can cause a decrease of up to the 70% of the ventilation rate in the central street. Further work will focus on extending this parametric analysis and extrapolating it to real cities.

Keywords: *Urban wind flow; Outdoor ventilation; CFD; Urban morphology.*

1 INTRODUCTION

Natural ventilation of urban areas is important for outdoor air quality and for the livability of the city. Different methods can be used to study urban wind flow, including reduced-scale and full-scale experiments and numerical simulation with Computational Fluid Dynamics (CFD). However, reduced-scale experiments can be limited by the choice of the model size and measurement resolution and by similarity requirements and scaling issues. Also the limited flexibility of experimental set-ups to study alternative geometrical and meteorological modifications can impose important constraints. Due to these limitations, CFD has increasingly emerged as a powerful tool to study urban wind flow and related problems (e.g. [Baik et al. 2000, Chang et al. 2003, Franke et al. 2007, Tominaga et al. 2008, Gousseau et al. 2011, Blocken et al. 2012, Ramponi and Blocken 2012a, 2012b]). CFD provides whole-field airflow data without similarity constraints and it allows efficient parametric studies for different geometrical and meteorological conditions.

However, verification and validation studies are imperative, which in turn requires high-quality experimental data.

Urban wind flow is strongly influenced by the urban morphology, i.e. the shape and dimensions of buildings and streets. The urban morphology can be described by several parameters, two of which are the plan area density (λ_P) and the frontal area density (λ_F). These are defined as the ratio between the plan and frontal building area and the lot surface (Figure 1a). They take into account the shape of the buildings and their mutual relations and are related to the different flow regimes introduced by Oke [1988], i.e. isolated obstacle flow, wake interference flow and skimming flow. The impact of the urban morphology on the wind flow can be evaluated by extending the concept of indoor ventilation efficiency indices to the outdoor ventilation, e.g. ventilation rate and mean age of air [Buccolieri et al. 2010].The present paper reports the first results of a CFD study of isothermal urban wind flow within simplified urban configurations, aimed at the assessment of outdoor ventilation. Nine different urban configurations are defined by varying the plan and frontal area density. Four of these configurations are used for a preliminary study and the first results are presented. The 3D steady RANS equations are solved using the Renormalization Group (RNG) k-ε turbulence model and the numerical results are compared with part of the extensive wind pressure database of the Tokyo Polytechnic University (TPU) [Quan et al. 2007a,b]. From these simulations, the outdoor ventilation rates are calculated and compared.

2   URBAN CONFIGURATIONS

Nine urban configurations are defined by varying the plan area density from 0.1 to 0.6 (Figure 1b) and the building height from 0.06 m to 0.18 m (Figure 1c), obtaining a variation of the frontal area density from 0.02 to 0.45. These nine urban configurations are chosen based on the measurements by Quan et al. [2007a,b] on reduced-scale urban models..

In this paper, only four of these nine configurations are analyzed, i.e. the ones with the lowest (case A) and highest (case C) plan area density and the smallest (H_1) and the highest (H_3) building models. The resulting frontal area densities for the mentioned cases are 0.02 for case A(H_1), 0.07 for case A(H_3), 0.15 for case C(H_1) and 0.45 for case C(H_3). The chosen configurations consist of flat-roof building models with uniform height and a fixed base area of L x W = 0.16 x 0.24 m². Simulations are made at reduced scale (wind tunnel scale).
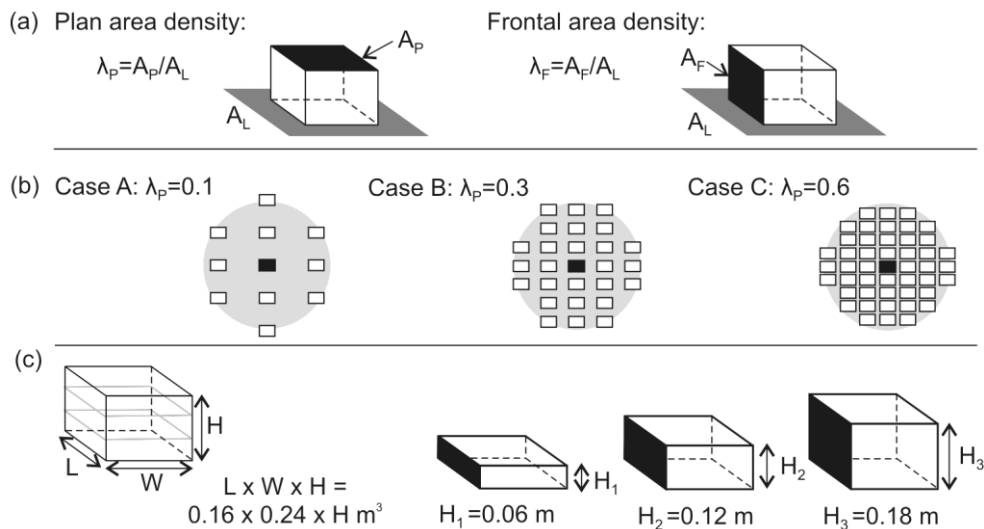

Figure 1. (a) Definition of plan area density and frontal area density; (b) variation of plan area density (λ_P) from 0.1 (case A) to 0.6 (case C); (c) variation of building height from 0.06 m (H_1) to 0.18 m (H_3).

3   EXPERIMENTAL DATA

Reduced-scale experiments were performed in the TPU atmospheric boundary layer (ABL) wind tunnel in Tokyo (Japan) on 111 urban configurations. The wind tunnel has a test section of 2.2 x 1.8 m². The geometric scale of the urban models was 1:100, while the velocity scale was assumed equal to 1:3. The mean wind speed and turbulence intensity profiles were measured at the center of the turntable without models present. The measured mean wind speed and turbulence intensity at the average-building height of 0.1 m were about 7.8 m/s and 0.25, respectively (Figure 2). At 0.5 m, the measured mean wind speed and turbulence intensity were about 12 m/s and 0.2, respectively. Figure 2 shows the measured profiles (black/gray symbols up to 0.5 m) and the extrapolated data above 0.5 m (white symbols and solid line). Further information about the wind tunnel tests are reported in Quan et al. [2007a,b] and in the online database.
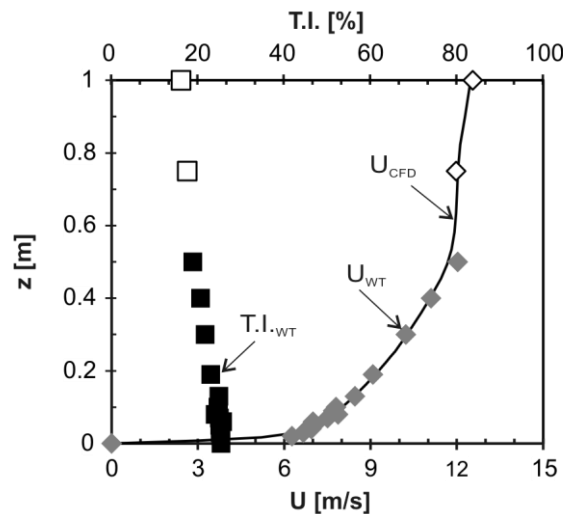

Figure 2. Vertical profiles of mean wind speed and turbulence intensity as measured in the wind tunnel (solid symbols) and as extrapolated from the wind tunnel data (open symbols and solid line).

4   NUMERICAL MODEL

4.1   Computational domain and grid

The computational domain and grid used for the numerical simulations were generated using the surface-grid extrusion technique presented by van Hooff and Blocken [2010] and in accordance with the best practice guidelines by Franke et al. [2007] and Tominaga et al. [2008]. In order to define a computational domain valid for each the four cases, an effective area of interest (Figure 3a) of 2.20 x 2.20 m² was first defined in which the four models are embedded. From this area, the required minimum distances of 5H from the inlet and the lateral right side of the domain and 15H from the outlet and left side of the domain were respected considering the maximum building height H_3. The geometry of the domain allows testing different wind directions (0° to 45°) in further steps of the analysis. The resulting reduced-scale domain size is L x W x H = 5.8 x 5.8 x1.08 m³.
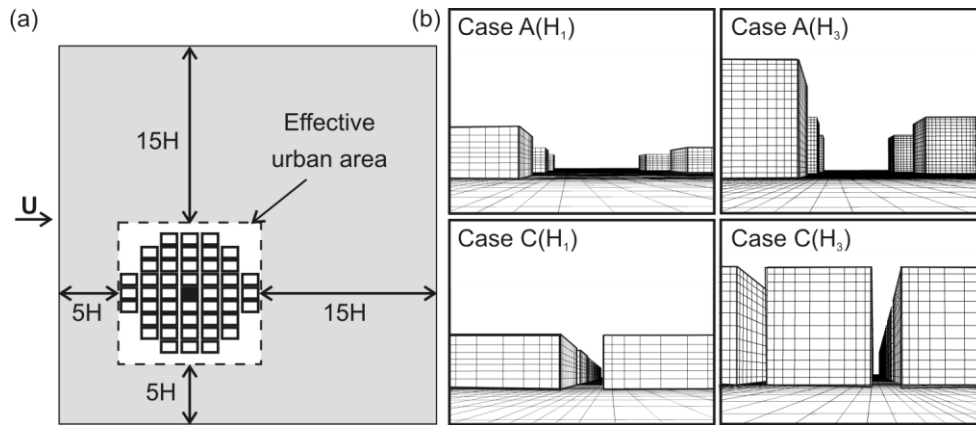
Figure 3. (a) Computational domain size for the cases $C(H_1)$ and $C(H_3)$; (b) Perspective view of the computational grids used for the simulations.

A grid sensitivity analysis was conducted for the cases $A(H_3)$ and $C(H_3)$ by refining and coarsening the basic grid by about a factor $\sqrt{2}$. The three grids tested consist of 562,334 cells (Coarse Grid), 836,115 cells (Base grid) and 1,280,928 cells (Fine grid). Results obtained with the different grids were compared in terms of the mean streamwise wind speed in the wake and the side of the central building and of mean pressure coefficient averaged on the central building surfaces. Figure 4 shows the results of the grid sensitivity analysis for the case $A(H_3)$. Since the results did not show a grid dependency for the mean wind speed, only the results of the mean pressure coefficients are reported. Based on the results of this analysis, the basic grid was chosen for the further simulations and similar grids were constructed for the other configurations. The resulting grids for the four cases consist of 747,335 cells for case $A(H_1)$, 836,115 cells for case $A(H_3)$, 852,768 cells for case $C(H_1)$ and 958,988 cells for case $C(H_3)$.
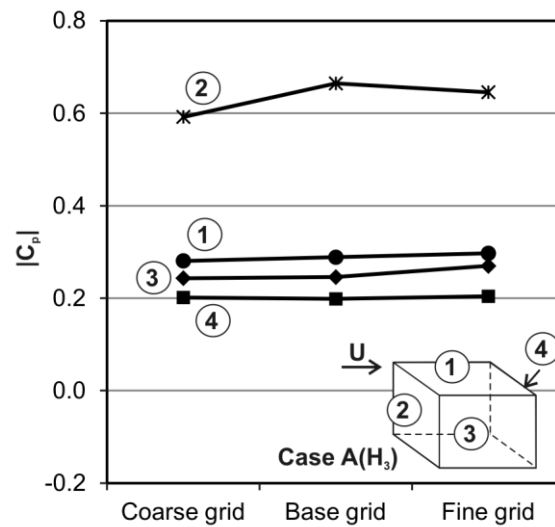

Figure 4. Grid sensitivity analysis for case $A(H_3)$: comparison between the absolute values of the mean wind pressure coefficients on the walls of the central building obtained with three grids.

4.2 Boundary conditions and solver settings

At the inlet of the domain, the vertical profiles of mean wind speed U, turbulent kinetic energy k and turbulence dissipation rate ε are imposed. The mean wind

speed profile is based on the experimental data (Figure 2). In the wind tunnel, high velocities are used to obtain Reynolds number independent flow. The building Reynolds numbers in this study range from 3.19×10^4 to 9.56×10^4. For the CFD study, the same conditions as in the wind tunnel are used. Although in reality, often much lower wind speeds will occur, the Reynolds number independence of the flow conditions does not compromise their representativeness, at least in isothermal situations.

The turbulent kinetic energy profile is calculated as $k = (I_u U)^2$, where I_u is the turbulence intensity. The turbulence dissipation rate is calculated using $\varepsilon = (u^*)^3/(\kappa(z + z_0))$, where κ is the von Karman constant (= 0.42), z the height coordinate, u^* the friction velocity (= 0.484 m/s) and z_0 the aerodynamic roughness length (= 0.002 m). Note that u^* and z_0 are obtained based on fitting a logarithmic profile to the experimental data of the mean wind speed. For the ground plane, the standard wall functions by Launder and Spalding [1974] with the sand-grain based roughness modification by Cebeci and Bradshaw [1977] are used. The values of the roughness parameters are determined using the relationship derived by Blocken et al. [2007], i.e. $k_s = (9.793 \, z_0)/C_s$. For the present cases, the equivalent sand-grain roughness height k_s is taken equal to 0.0045 m and the roughness constant C_s is 4.35. k_S of the building surfaces is assumed to be zero. Zero static pressure is imposed at the outlet. Symmetry boundary conditions are imposed at the top and lateral sides of the domain.

For the grid sensitivity study the 3D steady RANS equations are solved in combination with the standard k-ε turbulence model [Jones and Launder 1972]. However, a comparison between different turbulence models revealed that the (Renormalization Group) RNG k-ε model [Yakhot et al. 1992, Choudhury 1993] performed better for the selected cases. Thus, the latter model is used for the present study. The SIMPLE algorithm is used for pressure-velocity coupling, pressure interpolation is second order and second-order discretisation schemes are used for both the convection terms and the viscous terms of the governing equations. Convergence is achieved when all the scaled residuals levelled off and reach a minimum of 10^{-8} for y and z velocity, 10^{-7} for x velocity, k and ε, and 10^{-5} for continuity.

5   FIRST RESULTS

5.1   Comparison between numerical simulations and experiments

The numerical results for the case $A(H_3)$ are compared with the experiments in terms of the mean pressure coefficient along the midline of the surfaces of the central building (Figure 5). Given the limitations of steady RANS modeling for urban wind flow [Yoshie et al. 2007, Franke et al. 2007, Blocken et al. 2012], a fair overall agreement is reported. The discrepancies are attributed to the limitation of the RANS approach in accurately reproducing the separation zones downwind of the edges of the windward wall, both on the roof and on the lateral walls. Note however that the variables of interest for the calculation of the outdoor ventilation rate are velocities in the streets, rather than pressure coefficients. However, because no velocity data was available from the wind tunnel experiments, a validation based only on mean pressure coefficients was performed. It is important to note that previous studies have shown that RANS performs much better in predicting wind velocities in passages between buildings than in predicting pressure coefficients at building facades [Blocken et al. 2008, Nore et al. 2010]. Given the fair qualitative agreement in terms of mean pressure coefficients but especially given the known good performance of RANS in terms of mean velocities in passages between buildings, this model will be used for further analysis.
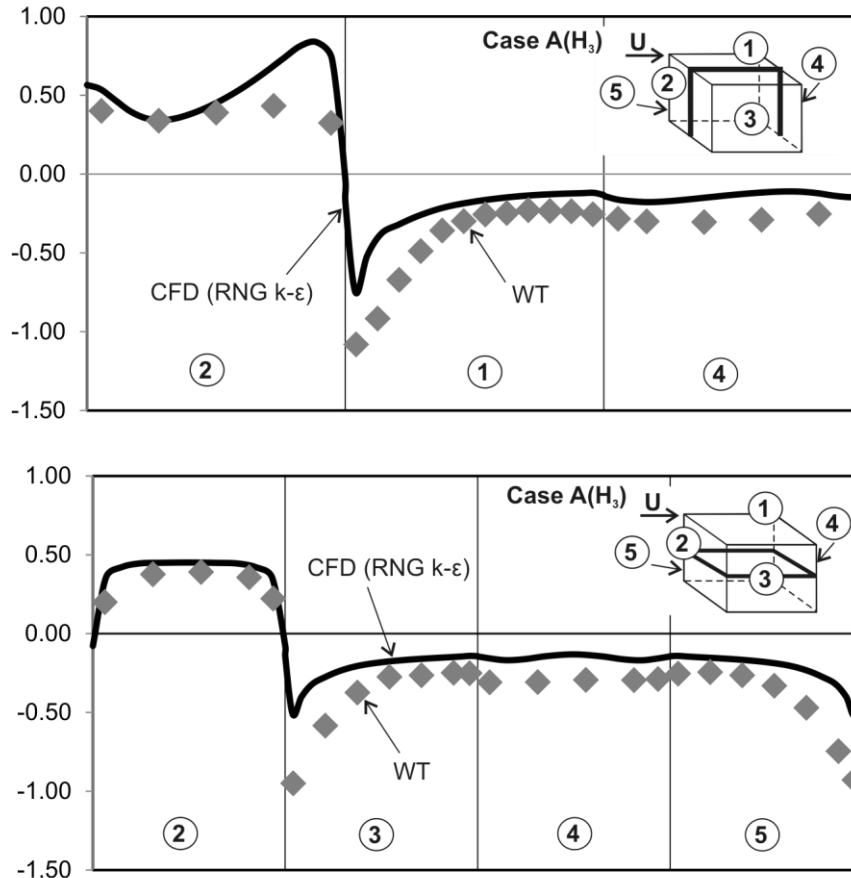
Figure 5. Comparison of numerical and experimental results for case $A(H_3)$ in terms of mean pressure coefficients along the midlines of the central building.

5.2 Results from the calculation of the ventilation rate

The ventilation rate $Q(x)$ in the street besides the central building is obtained as $Q(x)=\rho A U(x)$, where ρ is the air density, A is the cross-sectional area of the street, and $U(x)$ is the mean wind speed in the streamwise direction averaged over section A. For each configuration three positions along the street are considered (Fig. 6c), i.e. the first building position (x_0), and the inlet (x_{IN}) and outlet (x_{OUT}) of the control volume defined as in Fig. 6b at the central building position. The ratios of the local ventilation rates $Q(x_{IN})$ and $Q(x_{OUT})$ at the central building position divided by the ventilation rate $Q(x_0)$ at the first building position are compared to evaluate the effect of the presence of the upstream surrounding buildings on the development of the urban wind flow (Fig. 6a).

As shown in Figure 6, in the most sparse configurations $A(H_1)$ and $A(H_3)$ the influence of the upstream buildings is minimal and the ventilation rate decreases of about the 15% towards the central building. On the other hand, in the very dense configurations $C(H_1)$ and $C(H_3)$ the reduction of the ventilation rate due to the upstream buildings is very significant and rises up to about 70%. The unexpected increase of the ventilation rate close to the outlet of the street for the case $C(H_1)$ is attributed to the observed irregular influence of the flow on the top of the buildings, which is very strong for the ratio between the building height (0.06 m) and the street width (about 0.04 m), as shown in Figure 6c.
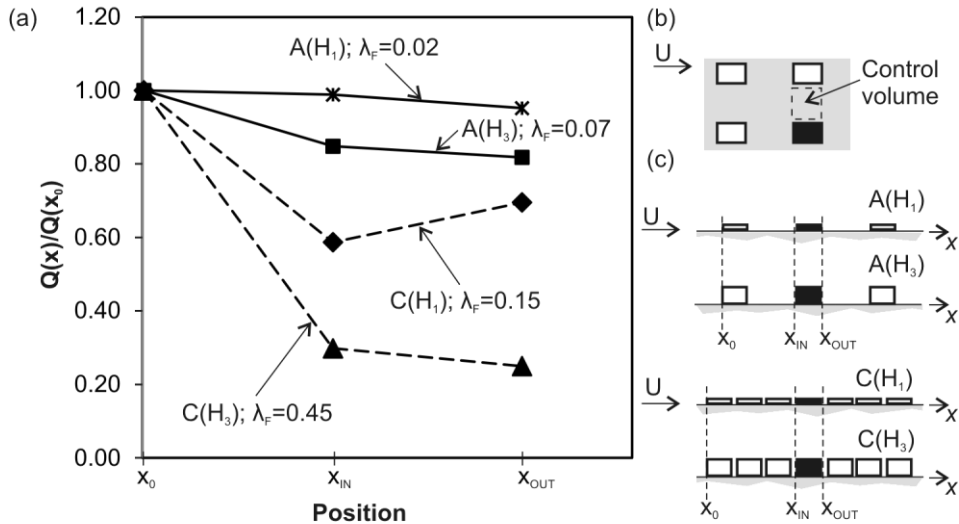
Figure 6. (a) Comparison of the ratio $Q(x)/Q(x_0)$ between the ventilation rates at the first and the central building positions; (b) Definition of a control volume of interest, ground plane; (c) Sections used for calculating the ventilation rate in the different urban configurations, vertical section.

6 DISCUSSION AND CONCLUSIONS

The first results of a CFD study on the influence of urban morphology on outdoor ventilation were shown in this paper. Four urban configurations were defined by varying the plan and frontal area densities from 0.1 to 0.6, and from 0.02 to 0.45, respectively. The 3D steady RANS equations closed by the RNG k-ε turbulence model were solved and the results were compared with experiments. The ventilation rate along a central street was calculated to evaluate the influence of the upstream buildings on the outdoor ventilation rates.

A fair overall good agreement was found between experimental and numerical results. The analysis of the ventilation ratios points out that the effect of the upstream buildings in the sparse configurations (case A) is rather limited and up to 15%, while for the dense configurations (case C) it is large and rises up to 70%. The influence of the flow on the top of the buildings might be relevant for the very low-rise buildings in a dense configuration (case $C(H_1)$) and should be investigated further. In the near future, a parameterization of the ventilation flow rates in terms of building height, and plan and frontal area density will be attempted, building further on the concept of "building scaling length" [Wilson et al. 1989]. Furthermore, an extensive parametric study will address a wider range of urban configurations.

ACKNOWLEDGMENTS

REFERENCES

Baik, J.J., R.S. Park, H.Y. Chun, and J.J. Kim, A laboratory model of urban-street canyon flows. *Journal of Applied Meteorology*, 39, 1592-1600, 2000.

Blocken, B., P. Moonen, T. Stathopoulos, and J. Carmeliet, A numerical study on the existence of the Venturi-effect in passages between perpendicular buildings. *Journal of Engineering Mechanics - ASCE* 134(12), 1021-1028, 2008.

Blocken, B., W. Janssen, and T. van Hooff, CFD simulation for pedestrian wind comfort and wind safety in urban areas: General decision framework and case

study for the Eindhoven University campus, *Environmental Modelling & Software*, 30, 15–34, 2012.

Blocken, B., T. Stathopoulos, and J. Carmeliet, CFD simulation of the atmospheric boundary layer: wall function problems, *Atmospheric Environment*, 41, 238-252, 2007.

Buccolieri, R., M. Sandberg, and S. Di Sabatino, City breathability and its link to pollutant concentration distribution within urban-like geometries, *Atmospheric Environment*, 44, 1894-1903, 2010.

Cebeci, T., and P. Bradshaw, *Momentum Transfer in Boundary Layers,* Hemisphere Publishing Corp, New York, 1977.

Chang, C.H., and R.N. Meroney, The effect of surroundings with different separation distances on surface pressures on low-rise buildings, *Journal of Wind Engineering and Industrial Aerodynamics*, 91, 1039–1050, 2003.

Choudhury, D., *Introduction to the renormalization group method and turbulence modelling*, Technical Memorandum TM-107, 1993.

Franke, J., A. Hellsten, H. Schlünzen, and B. Carissimo, *Best practice guideline for the CFD simulation of flows in the urban environment*, COST 732: Quality Assurance and Improvement of Microscale Meteorological Models, 2007.

Gousseau, P., B. Blocken, T. Stathopoulos, and G.J.F. van Heijst, CFD simulation of near-field pollutant dispersion on a high-resolution grid: A case study by LES and RANS for a building group in downtown Montreal, *Atmospheric Environment*, 45, 428-438, 2011.

Jones, W., and B. Launder, The prediction of laminarization with a two-equation model of turbulence, *International Journal of Heat and Mass Transfer*, 15, 301-314, 1972.

Launder, B.E., and D.B. Spalding, The numerical computation of turbulent flows. *Computer Methods in Applied Mechanics and Engineering*, 3, 269-289, 1974.

Nore, K., B. Blocken, and J.V. Thue, On CFD simulation of wind-induced airflow in narrow ventilated facade cavities: coupled and decoupled simulations and modelling limitations. *Building and Environment* 45(8), 1834-1846, 2010.

Oke, T., Street design and urban canopy layer climate, *Energy and Buildings*, 11, 103-113, 1988.

Quan, Y., Y. Tamura, M. Matsui, S. Cao, A. Yoshida, and S. Xu, Interference effect of a surrounding building group on wind loads on flat roof of low-rise building: Part I, Distribution of local wind pressure coefficient, *Wind Engineers, JAVE*, 32, 211-212, 2007a.

Quan, Y., Y. Tamura, M. Matsui, S. Cao, A. Yoshida, and S. Xu, Interference effect of a surrounding building group on wind loads on flat roof of low-rise building: Part II, Interference factor of worst extreme local and area-averaged suction pressure coefficients, *Wind Engineers, JAVE*, 32, 213-214, 2007b.

Ramponi, R., and B. Blocken, CFD simulation of cross-ventilation for a generic isolated building: Impact of computational parameters, *Building and Environment*, 53, 34-48, 2012a.

Ramponi, R., and B. Blocken, CFD simulation of cross-ventilation flow for different isolated building configurations: validation with wind tunnel measurements and analysis of physical and numerical diffusion effects. *Journal of Wind Engineering and Industrial Aerodynamics*. In press. 2012b.

Tominaga, Y., A. Mochida, R. Yoshie, H. Kataoka, T. Nozu, M. Yoshikawa, and T. Shirasawa, AIJ guidelines for practical applications of CFD to pedestrian wind environment around buildings, *Journal of Wind Engineering and Industrial Aerodynamics*, 96, 1749-1761, 2008.

van Hooff, T., and B. Blocken, Coupled urban wind flow and indoor natural ventilation modelling on a high-resolution grid: A case study for the Amsterdam ArenA stadium, *Environmental Modelling & Software*, 25(1), 51-65, 2010.

Xie, Z.T., O. Coceal, and I.P. Castro, Large-eddy simulation of flows over random urban-like obstacles, *Boundary-Layer Meteorology*, 129, 1-23, 2008.

Yakhot, V., S.A. Orszag, S. Thangam, T.B. Gatski, and C.G. Speziale, Development of turbulence models for shear flows by a double expansion technique, *Physics of Fluids*, 4, 1510-1520, 1992.

Yoshie, R., A. Mochida, Y. Tominaga, H. Kataoka, K. Harimoto, T. Nozu, and T., Shirasawa, Cooperative project for CFD prediction of pedestrian wind environment in the Architectural Institute of Japan, *Journal of Wind Engineering and Industrial Aerodynamics*, 95, 1551-1578, 2007.

Wilson, D.J., *Airflow around buildings*, ASHRAE Handbook of Fundamentals, 14.1 –14.18, 1989.